

Investigation of the ^{10}Li shell inversion by neutron continuum transfer reaction

M. Cavallaro,¹ M. De Napoli,^{2,*} F. Cappuzzello,^{1,3} S. E. A. Orrigo,⁴ C. Agodi,¹ M. Bondí,²
D. Carbone,¹ A. Cunsolo,¹ B. Davids,⁵ T. Davinson,⁶ A. Foti,^{2,3} N. Galinski,⁵ R. Kanungo,⁷
H. Lenske,⁸ C. Ruiz,⁵ and A. Sanetullaev⁵

¹INFN—Laboratori Nazionali del Sud, I-95123 Catania, Italy

²INFN—Sezione di Catania, I-95123 Catania, Italy

³Dipartimento di Fisica e Astronomia, Università di Catania, I-95123 Catania, Italy

⁴Instituto de Física Corpuscular, CSIC-Universidad de Valencia, E-46071 Valencia, Spain

⁵TRIUMF, Vancouver, British Columbia V6T2A3, Canada

⁶School of Physics and Astronomy, University of Edinburgh, EH9 3FD Edinburgh, United Kingdom

⁷Astronomy and Physics Department, Saint Marys University, Halifax, Nova Scotia B3H 3C3, Canada

⁸Institut für Theoretische Physik, Universität Giessen, D-35392 Giessen, Germany

(Received 26 January 2016; revised manuscript received 5 May 2016; published 3 January 2017)

This Letter reports a study of the highly debated ^{10}Li structure through the $d(^9\text{Li}, p)^{10}\text{Li}$ one-neutron transfer reaction at 100 MeV. The ^{10}Li energy spectrum is measured up to 4.6 MeV and angular distributions corresponding to different excitation energy regions are reported for the first time. The comparison between data and theoretical predictions, including pairing correlation effects, shows the existence of a $p_{1/2}$ resonance at 0.45 ± 0.03 MeV excitation energy, while no evidence for a significant s -wave contribution close to the threshold energy is observed. Moreover, two high-lying structures are populated at 1.5 and 2.9 MeV. The corresponding angular distributions suggest a significant $s_{1/2}$ partial-wave contribution for the 1.5 MeV structure and a mixing of configurations at higher energy, with the $d_{5/2}$ partial-wave contributing the most to the cross section.

DOI: 10.1103/PhysRevLett.118.012701

When approaching the driplines, continuum spectroscopy is a demanding challenge to nuclear structure physics, both for experiment and theory. In this respect, ^{10}Li is a system of prime interest to understand the transition from bound to unbound nuclear configurations and investigate dissolution of nuclei at the neutron dripline. For example, knowing the ground-state dominant configuration can shine light onto the debate about the shell inversion between the $2s_{1/2}$ and the $1p_{1/2}$ orbitals in the $N = 7$ isotones. Studying the unbound ^{10}Li system is of great interest not only for nuclear continuum dynamics but also for understanding the formation of the two-neutron halo in ^{11}Li [1–4]. Its description, either in cluster models or in quasiparticle approaches, relies in fact on the interaction between the neutrons and the ^9Li core [5].

In this Letter we report new measurements of the $d(^9\text{Li}, p)^{10}\text{Li}$ one-neutron transfer reaction performed at $E_{\text{Lab}} = 100$ MeV incident energy.

Previous experiments investigated the ^{10}Li structure through various techniques. Fragmentation from ^{18}O [6,7], one- and two-particle removal from ^{11}Be , ^{11}Li and ^{12}B [8–13], multineutron transfer [14–19] and stopped pion absorption reactions [20] have added significant information to the knowledge of the ^{10}Li nucleus thanks to their different selectivity. Most of the studies report on the presence of a $p_{1/2}$ neutron resonance peaked at around 500–700 keV, with the possible population of the other

member of the doublet at about 100–200 keV [12,16,18]. Some of these works agreed on the presence of an s -wave virtual state close to the threshold with a scattering length in the range from -20 to -30 fm [7,8,10,11]. Very little information exists on the neutron d -wave [11,15]. However, the conclusions are often weakened by poor statistics and sometimes the quantum number assignments are based only on the shape of the resonances measured over a background.

In this scenario a key role is played by one-neutron transfer reactions, which are appropriate tools for continuum spectroscopy since they probe single-neutron components of the nuclear wave function. The $d(^9\text{Li}, p)^{10}\text{Li}$ transfer reaction in inverse kinematics was successfully used at Radioactive beam EXperiment-Isotope Separator On Line DEvice (REX-ISOLDE) [21] and, at about the same time, at National Superconducting Cyclotron Laboratory (NSCL) [22] to obtain spectral and angular distributions for $^9\text{Li} + n$ continuum states. Those data were also analyzed in [23], describing the spectral distributions in the single particle continuum by an extended microscopic mean-field approach and applying Distorted Wave Born Approximation (DWBA) methods for the population of unbound states in transfer reactions. However the low statistics and the poor energy resolution prevented definitive conclusions on the ^{10}Li puzzle from being drawn. Thus, despite the significant amount of experimental efforts

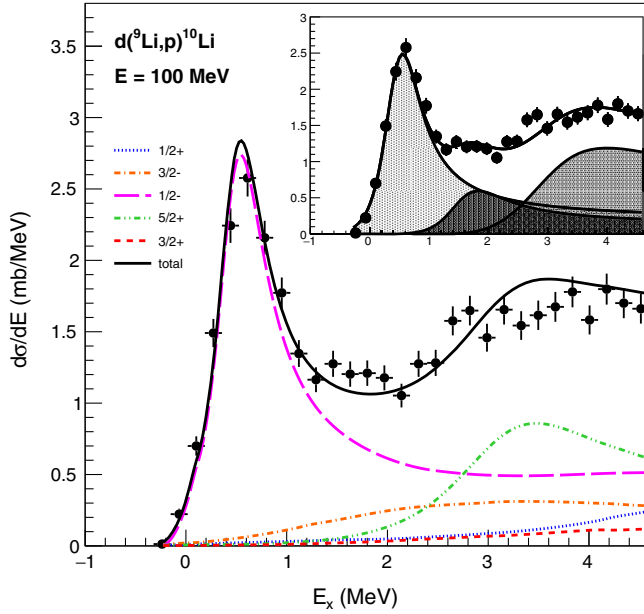


FIG. 1. ^{10}Li energy spectrum for the $d(^9\text{Li}, p)^{10}\text{Li}$ reaction at 100 MeV incident energy and $\theta_{CM} = [5.5^\circ, 16.5^\circ]$. The curves show the partial wave contributions obtained by theoretical calculations, the sum of which is indicated by the solid black line. The best-fitting sum of three Fano functions convoluted with the experimental energy resolution is shown in the inset.

carried out in the past, the properties of ^{10}Li remain unclear to such an extent that even the ground state energy and spin-parity assignment is controversial. The ^{10}Li level scheme at high excitation energy is even more obscure, due to the rather poor experimental information. The situation is ambiguous also on the theoretical side, with some calculations predicting a p -wave [15,17,24–26] and others an s -wave dominance at the lowest energy [27–30].

In our $d(^9\text{Li}, p)^{10}\text{Li}$ experiment, the ^9Li beam intensity (10^6 pps) of the TRIUMF ISAC-II facility [31], much higher than those used in all the previous experiments [21,22], allowed us to reconstruct the ^{10}Li excitation energy spectrum with almost 2 orders of magnitude higher statistics compared to [21,22]. The recoil protons and the ^9Li nuclei produced by the ^{10}Li breakup were detected in coincidence by a system of highly segmented silicon-strip detectors at the TRIUMF U.K. Detector Array (TUDA) facility. In order to detect and identify the ^9Li emitted at very forward angles $\theta_{\text{lab}} = [1.0^\circ, 3.4^\circ]$, a $\Delta E - E$ telescope made by two 500 μm thick S2-style radial strip detectors was placed 59.6 cm downstream of a $126 \pm 1 \mu\text{g}/\text{cm}^2$ CD_2 target. The energy and emission angle of the recoil protons were measured by the Louvain-Edinburgh Detector Array (LEDA) setup [32] made by eight YY1-style strip detectors arranged in a flat annular configuration. LEDA was placed 9.9 cm upstream of the target to cover the backward angular region $\theta_{\text{lab}} = [127^\circ, 161^\circ]$, corresponding to ^{10}Li emitted within $\theta_{CM} = [5.5^\circ, 16.5^\circ]$.

The beam current was measured by a Faraday cup whose accuracy was determined by elastic scattering measurements.

For those events where a ^9Li was observed in coincidence with a signal in the LEDA detectors, the ^{10}Li excitation energies $E_x = Q_0 - Q$ (where Q_0 is the ground to ground state Q value) were obtained by the missing mass determination based on relativistic kinematic transformations. The spectrum integrated over the covered angular region is shown in Fig. 1. The uncertainty on the angle (from 0.5° for the inmost strip to 1.1° for the outmost one) and the energy resolution (30 keV FWHM for α particles of 5.486 MeV) of the LEDA system result in an overall uncertainty in the reconstructed excitation energy of about 200 keV (FWHM). Absolute cross sections are measured with a systematic uncertainty of 15% resulting from the beam current and target thickness uncertainties. The statistical error, shown as error bars in Figs. 1 and 2, is about 15%.

First we analyze the measured energy spectrum on empirical grounds by using three Fano functions [33,34] convoluted with the experimental energy resolution (Fig. 1, inset). The Fano approach predicts a transfer cross section of the form

$$\sigma = \sigma_{\text{cont}} \frac{|q + \epsilon|^2}{1 + \epsilon^2} \quad (1)$$

where σ_{cont} denotes the transfer cross section into the continuum and $\epsilon = 2(E - E_r)/\Gamma_r$ is given by the energy E_r and the decay width Γ_r of the resonance. The line shape is controlled by the Fano parameter q . Except for a phase, it is determined by the population probability of the resonance over the continuum component, as discussed, e.g., in Ref. [35]. For $q \gg 1$, the line shape approaches a Lorentz curve, recovering the usually assumed Breit-Wigner spectral distribution. Physically, that situation is met by a reaction preferentially populating the ^{10}Li resonant component, thus suppressing the excitation of the nonresonant $n + ^9\text{Li}$ background. Applying this scheme to the measured spectral distribution, a resonance at $E_r = 0.45 \pm 0.03$ MeV with $\Gamma_r = 0.68 \pm 0.03$ MeV and $q = 3.7 \pm 0.6$, together with a second one at $E_r = 1.5 \pm 0.1$ MeV with $\Gamma_r = 1.1 \pm 0.3$ MeV and $q = 2.1 \pm 0.3$, are extracted from the fit. At higher excitation energies, measured for the first time in a one-neutron transfer reaction, the data show the presence of a third structure at $E_r = 2.9 \pm 0.3$ MeV, with $\Gamma_r = 2.6 \pm 0.6$ MeV and $q = 1.2 \pm 0.3$. It is worth noticing that in general the energy of the resonant state in the Fano function does not coincide with the maximum of the cross section, which in our case is located at 0.55 MeV, 1.9 MeV, and 3.9 MeV for the three observed peaks.

As shown in Fig. 1, the measured cross section drops to zero near the threshold, where it is entirely well reproduced by the 0.45 MeV resonance without any need of introducing additional near-threshold strength, as for instance in

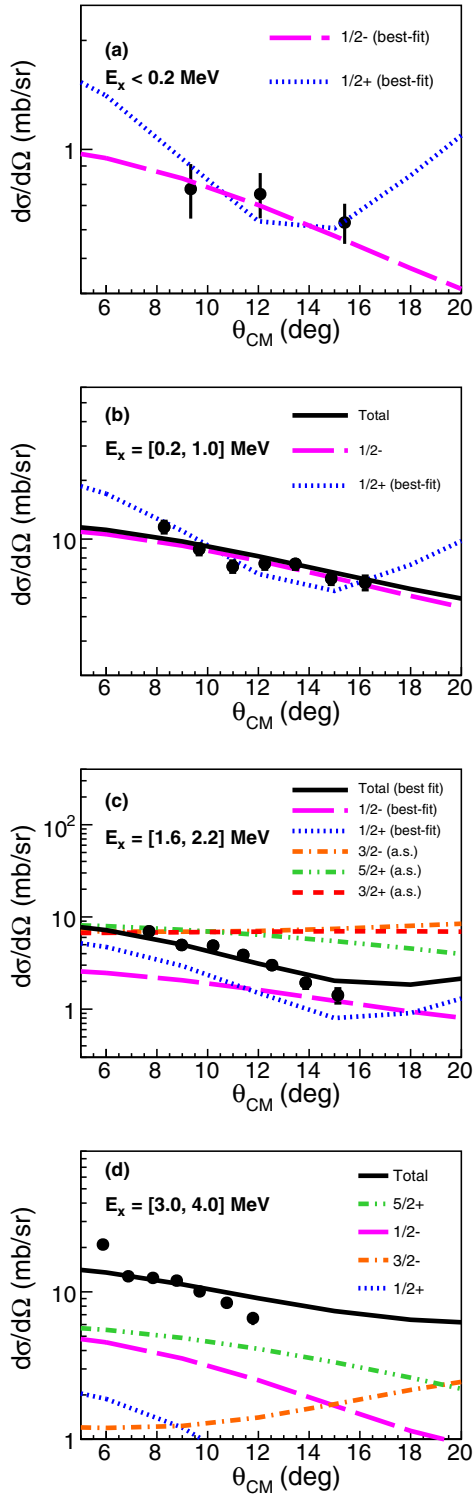


FIG. 2. Angular distributions for the $d(^9\text{Li}, p)^{10}\text{Li}$ reaction integrated over (a) $E_x < 0.2$ MeV, (b) $E_x = [0.2, 1.0]$ MeV, (c) $E_x = [1.6, 2.2]$ MeV, and (d) $E_x = [3.0, 4.0]$ MeV. In (a), data have been grouped in three angular bins to allow for significant statistics. The curves are the calculated partial wave contributions integrated over the same energy range. Figure legends indicate when curves have been arbitrarily scaled (a.s.) or scaled using a best-fit procedure (best-fit).

Ref. [21]. Clearly this best fit does not rule out the presence of other states in this region. However, if a hypothetical low-lying state is supposed to be present under the main resonance, its contribution to the cross section is anyhow expected to be strongly limited. For example, by artificially introducing a fourth Fano function centered at 0.1 MeV, the best-fit quality is preserved if the maximum strength of this additional low-lying state is 18% (4%) of the main-peak one in the energy region $E_x < 0.3$ MeV ($E_x < 4.6$ MeV).

Figure 2 shows the angular distributions for the near-threshold region $E_x < 200$ keV and for the energy intervals where the three observed structures are peaked. Their different slopes confirm the sensitivity of the measured reaction to angular momentum transfer and thus the possibility to extract spectroscopic information in different regions of the excitation energy spectrum.

Excitation energies and angular distributions are compared with the theoretical predictions of the model developed in Ref. [23] and already used to analyze the REX-ISOLDE results [21]. This model is based on an extended microscopic mean-field approach which includes pairing-type correlations across the particle emission threshold. In fact pairing effects from particle-particle interactions play a fundamental role in continuum spectroscopy and strongly influence the low-energy continuum of unbound nuclei. The problem is adequately formulated in terms of the Gorkov equations replacing the Bardeen-Cooper-Schrieffer (BCS) approximation by a set of coupled channels equations [23]. As a consequence, the single particle mean-field acquires a pairing self-energy which is nonlocal and energy dependent. Continuum states are affected in a particular manner. As discussed in detail in Ref. [23], the pairing field induces an additional phase shift which, under appropriate circumstances, leads to a new type of pairing-assisted mean-field resonances, resembling the Fano resonance mechanism [35]. Qualitatively, both the purely phenomenological Fano analysis and the microscopic results agree in that both predict the prevalence of populating particle-type open channel configurations as indicated by $q > 1$. This dynamical mechanism is a universal feature of all open quantum systems. The structure results are used as an input for single-nucleon transfer reaction calculations populating unbound states in ^{10}Li . The $d + ^9\text{Li} \rightarrow p + ^{10}\text{Li}$ transfer reaction is described by DWBA calculations following closely the approach in [23], but updated to the present higher incident energy. In order to account globally for dynamical core polarization (see below) we have introduced an additional polarization potential.

The data compared to the theoretical results folded with experimental resolution show a number of interesting features, shedding new light on the long-standing uncertainties on the level structure of neutron-rich Li isotopes.

Figure 1 shows that the model reproduces the energy spectrum below 200 keV with the $p_{1/2}$ partial-wave contribution (dashed pink curve). In addition to the model

prediction, we performed a shape analysis of the corresponding angular distribution to investigate the possible presence of additional near-threshold s -wave strength. The angular distribution was fitted with different curves corresponding to a pure $p_{1/2}$ orbital, a pure $s_{1/2}$ orbital, and a mixture of the two. The best fit performed with the pure $p_{1/2}$ orbital [dashed pink curve of Fig. 2(a)] returns a chi-square of 0.8, whereas the use of a pure $s_{1/2}$ orbital [dashed blue curve of Fig. 2(a)] returns a chi-square of 2.8. Mixing the two curves with free weights, the best-fit procedure returns a 100% p -wave configuration. Therefore, although the presence of an arbitrarily small s -wave contribution cannot be completely ruled out, the model, the data (cross sections rapidly dropping to zero at $E = 0$), and the best-fit analysis of both energy spectrum and angular distribution shape favor the $p_{1/2}$ orbital and a negligible s -wave contribution near the threshold.

The angular distribution for the 0.45 MeV resonance [Fig. 2(b)] is reproduced by the $p_{1/2}$ orbital confirming the observation of many other experiments and the Gorkov–Hartree-Fock-Bogoliubov (HFB) calculation reported in [23]. For the sake of comparison, we also report the result of the best fit performed with a pure $s_{1/2}$ orbital [blue dashed curve of Fig. 2(b)] although it shows a worse agreement with the data.

The 1.5 MeV resonance is not predicted by the model. However, the shape of the corresponding angular distribution [Fig. 2(c)] suggests an important s -wave contribution. The result of a fit performed by using a mixture of 51% p -wave and 49% s -wave is shown in Fig. 2(c) (black curve). The relative p and s strengths used in the fit are extracted from the corresponding Fano function analysis shown in the inset of Fig. 1, integrated over $1.6 \text{ MeV} < E_x < 2.2 \text{ MeV}$. Possible contributions from the $3/2^+$, $3/2^-$, and $5/2^+$ orbitals can be considered secondary since the shape of their angular distributions [arbitrarily scaled in Fig. 2(c) for comparison] is significantly different from the measured one.

Finally, the angular distribution of the $E_x = 2.9 \text{ MeV}$ structure [Fig. 2(d)] supports a mixing of configurations. According to the model the d -wave is the main contributor, as predicted in [23] where an $n + {}^9\text{Li } 5/2^+$ resonance was assigned to that region. The presence of d -wave strength at high excitation energies is also discussed in Ref. [36]. At the same time, the shape of the distribution indicates that adding more s -wave strength would improve the agreement between data and model predictions.

A comparison with the $d({}^{10}\text{Be}, p){}^{11}\text{Be}$ reaction at 21.4 MeV of Ref. [37] adds interesting information. Cross sections comparable with the present experiment are measured for the s and p resonances. This is expected assuming that (d, p) reactions are weakly influenced by the additional proton in ${}^{11}\text{Be}$. However, a suppression of the d -wave resonance is found in our data, indicating that the major part of the $d_{5/2}$ strength must be located above the explored energy interval.

On first sight, the spectrum seems to be dominated by the single-particle features of $n - {}^9\text{Li}$ scattering, in particular, because the (d, p) transfer reaction will populate primarily such doorway states. However, a closer inspection of the spectral distribution reveals a more subtle picture. The $1/2^-$ resonance carries 55% of the full single particle strength, similarly to the value obtained for the neutron p orbital in ${}^{11}\text{Be}$ [37]. The $5/2^+$ resonance appears to be a low-energy satellite with only 5% of the strength of a $5/2^+$ single-neutron resonance which theoretically is obtained outside the measured energy window. Thus, both states show considerable core polarization effects. Also the $1/2^+$ state carries only a small fraction of the single particle strength, indicating that it cannot be a pure single particle resonance structure, being excluded already for obvious reasons because the mean field alone does not support s -wave neutron resonances. The observed state must therefore contain a considerable amount of polarization dynamics producing a self-energy which gives rise to the observed spectral shape. The primary source of core polarization is the coupling to the ${}^9\text{Li } 2^+$ first excited state at 2.69 MeV. The induced self-energies will lead to energy shifts and new poles in propagators even below the kinematical threshold, moving part of the continuum strength downward.

Finally the spectra indicate another peculiarity of continuum spectroscopy visible in the width of the observed states. Obviously, below the core polarization threshold, imaginary self-energy parts, responsible for the damping width, do not contribute. Hence, below $E_x \sim 2.69 \text{ MeV}$ the width of the states reflects the branching ratio into the $n + {}^9\text{Li}$ elastic scattering channel superimposed on the width of elastic scattering resonances in those channels where they exist. Interestingly, a similar effect was found some time ago in ${}^{19}\text{C}$ when studying one-neutron removal reactions. For that nucleus the data analysis showed that core polarization-induced self-energies provide additional attraction as the major source of binding [38–40].

If our conclusions from the data are correct, the continuum level sequence in ${}^{10}\text{Li}$ still seems to follow the order known from bound states in stable nuclei, namely, first populating primarily the p -shell, followed by the (s, d) -shell, but with the caveat that considerable fractions of spectral strength are distributed over a wider energy window. Hence, the spectra still contain traces of the shell structure anticipated in a fictitious stable nucleus of this mass and charge but embedded into a considerable background of fragmented intruder components. In that respect the situation resembles other neutron-rich nuclei, where level inversions are a frequent observation, as in the so-called *island of inversion* around ${}^{32}\text{Mg}$ [41,42].

In conclusion, in this letter we have reported the first measurement of the ${}^{10}\text{Li}$ energy spectrum up to 4.6 MeV obtained with significant statistics by the $d({}^9\text{Li}, p){}^{10}\text{Li}$ one-neutron transfer reaction. The angular distributions corresponding to different excitation energy regions were also

measured and discussed. The data clearly show the presence of a $p_{1/2}$ resonance at $E_x = 0.45$ MeV whereas there is no strong evidence for a near-threshold s state. On the other hand, the shape of the angular distribution for the second bump at $E_x = 1.5$ MeV indicates a significant $s_{1/2}$ contribution. A third structure containing a relevant $d_{5/2}$ component is observed for the first time at $E_x = 2.9$ MeV. Beside the important core polarization effects and the dissolution of the shell structure in the continuum highlighted by the theoretical analysis, the absence of clear evidence of an s state at low energy in the data indicates that the level sequence in the ^{10}Li system may not show the shell inversion features observed in other $N = 7$ isotones such as ^{11}Be .

The authors acknowledge the Spanish MICINN Grants No. FPA2011-24553 and No. FPA2014-52823-C2-1-P; Centro de Excelencia Severo Ochoa del IFIC SEV-2014-0398; JuntaparalaAmpliacióndeEstudios Programme (CSIC JAE-Doc contract) co-financed by FSE; the support of the UK Science and Technology Facilities Council (STFC); the support of the Helmholtz International Center for FAIR for a research visit of S. E. A. O. to Giessen; and the support of the Natural Sciences and Engineering Research Council of Canada. TRIUMF receives federal funding via a contribution agreement through the National Research Council of Canada.

*marzio.denapoli@ct.infn.it

- [1] S. Shimoura, T. Nakamura, M. Ishihara, N. Inabe, T. Kobayashi, T. Kubo, R. H. Siemssen, I. Tanihata, and Y. Watanabe, *Phys. Lett. B* **348**, 29 (1995).
- [2] A. A. Korshennikov *et al.*, *Phys. Rev. C* **53**, R537 (1996).
- [3] I. Tanihata *et al.*, *Phys. Rev. Lett.* **100**, 192502 (2008).
- [4] R. Kanungo *et al.*, *Phys. Rev. Lett.* **114**, 192502 (2015).
- [5] M. V. Zhukov, B. V. Danilin, D. V. Fedorov, J. M. Bang, I. J. Thompson, and J. S. Vaagen, *Phys. Rep.* **231**, 151 (1993).
- [6] R. A. Kryger *et al.*, *Phys. Rev. C* **47**, R2439 (1993).
- [7] M. Thoennessen *et al.*, *Phys. Rev. C* **59**, 111 (1999).
- [8] M. Zinser *et al.*, *Phys. Rev. Lett.* **75**, 1719 (1995).
- [9] T. Kobayashi, K. Yoshida, A. Ozawa, I. Tanihata, A. Korshennikov, E. Nikolski, and T. Nakamura, *Nucl. Phys.* **A616**, 223c (1997).
- [10] M. Chartier *et al.*, *Phys. Lett. B* **510**, 24 (2001).
- [11] H. Simon *et al.*, *Nucl. Phys.* **A791**, 267 (2007).
- [12] J. K. Smith *et al.*, *Nucl. Phys.* **A940**, 235 (2015).
- [13] A. Sanetullaev *et al.*, *Phys. Lett. B* **755**, 481 (2016).
- [14] K. H. Wilcox, R. B. Weisenmiller, G. J. Wozniak, N. A. Jelley, D. Ashery, and J. Cerny, *Phys. Lett.* **59B**, 142 (1975).
- [15] H. G. Bohlen *et al.*, *Z. Phys. A* **344**, 381 (1993).
- [16] B. M. Young *et al.*, *Phys. Rev. C* **49**, 279 (1994).
- [17] H. G. Bohlen, W. von Oertzen, Th. Stolla, R. Kalpakchieva, B. Gebauer, M. Wilpert, Th. Wilpert, A. N. Ostrowski, S. M. Grimes, and T. N. Massey, *Nucl. Phys.* **A616**, 254c (1997).
- [18] H. G. Bohlen, A. Blazevic, B. Gebauer, W. Von Oertzen, S. Thummerer, R. Kalpakchieva, S. M. Grimes, and T. N. Massey, *Prog. Part. Nucl. Phys.* **42**, 17 (1999).
- [19] J. A. Caggiano, D. Bazin, W. Benenson, B. Davids, B. M. Sherrill, M. Steiner, J. Yurkon, A. F. Zeller, and B. Blank, *Phys. Rev. C* **60**, 064322 (1999).
- [20] B. A. Chernysev, Yu. B. Gurov, L. Yu. Korotkova, S. V. Lapushkin, R. V. Pritula, and V. G. Sandukovsky, *Int. J. Mod. Phys. E* **24**, 1550004 (2015).
- [21] H. B. Jeppesen *et al.*, *Phys. Lett. B* **642**, 449 (2006).
- [22] P. Santi *et al.*, *Phys. Rev. C* **67**, 024606 (2003).
- [23] S. E. A. Orrigo and H. Lenske, *Phys. Lett. B* **677**, 214 (2009).
- [24] K. Kato and K. Ikeda, *Prog. Theor. Phys.* **89**, 623 (1993).
- [25] J. Wurzer and H. M. Hofmann, *Z. Phys. A* **354**, 135 (1996).
- [26] P. Descouvemont, *Nucl. Phys.* **A626**, 647 (1997).
- [27] F. C. Barker and G. T. Hickey, *J. Phys. G* **3**, L23 (1977).
- [28] N. A. F. M. Poppelier, A. A. Wolters, and P. W. M. Glaudemans, *Z. Phys. A* **346**, 11 (1993).
- [29] I. J. Thompson and M. V. Zhukov, *Phys. Rev. C* **49**, 1904 (1994).
- [30] F. M. Nunes, I. J. Thompson, and R. C. Johnson, *Nucl. Phys.* **A596**, 171 (1996).
- [31] P. Bricault, *Eur. Phys. J. Spec. Top.* **150**, 227 (2007).
- [32] T. Davinson *et al.*, *Nucl. Instrum. Methods Phys. Res., Sect. A* **454**, 350 (2000).
- [33] U. Fano, *Phys. Rev.* **124**, 1866 (1961).
- [34] C. Ott, A. Kaldun, P. Raith, K. Meyer, M. Laux, J. Evers, C. H. Keitel, C. H. Greene, and T. Pfeifer, *Science* **340**, 716 (2013).
- [35] S. E. A. Orrigo, H. Lenske, F. Cappuzzello, A. Cunsolo, A. Foti, A. Lazzaro, C. Nociforo, and J. S. Winfield, *Phys. Lett. B* **633**, 469 (2006).
- [36] G. Blanchon, A. Bonaccorso, D. M. Brink, and N. Vinh Mau, *Nucl. Phys.* **A791**, 303 (2007).
- [37] K. T. Schmitt *et al.*, *Phys. Rev. C* **88**, 064612 (2013).
- [38] T. Baumann *et al.*, *Phys. Lett. B* **439**, 256 (1998).
- [39] H. Lenske, F. Hofmann, and C. M. Keil, *Prog. Part. Nucl. Phys.* **46**, 187 (2001).
- [40] D. Cortina-Gil *et al.*, *Eur. Phys. J. A* **10**, 49 (2001).
- [41] C. Detraz, D. Guillemaud, G. Huber, R. Klapisch, M. Langevin, F. Naulin, C. Thibault, L. C. Carraz, and F. Touchard, *Phys. Rev. C* **19**, 164 (1979).
- [42] D. Guillemaud-Mueller, C. Detraz, M. Langevin, F. Naulin, M. de Saint-Simon, C. Thibault, F. Touchard, and M. Epherre, *Nucl. Phys.* **A426**, 37 (1984).